Tmem178 acts in a novel negative feedback loop targeting NFATc1 to regulate bone mass

Corinne E. Decker[a,b], Zhengfeng Yang[a], Ryan Rimer[c], Kyung-Hyun Park-Min[d], Claudia Macaubas[e], Elizabeth D. Mellins[e], Deborah V. Novack[c], and Roberta Faccio[a,1]

[a]Department of Orthopaedic Surgery, Musculoskeletal Research Center, Washington University School of Medicine, St. Louis, MO 63110; [b]Graduate Program in Immunology, Division of Biology and Biomedical Sciences, Washington University in St. Louis, St. Louis, MO 63110; [c]Division of Bone and Mineral Diseases, Department of Medicine, Musculoskeletal Research Center, Washington University School of Medicine, St. Louis, MO 63110; [d]Arthritis and Tissue Degeneration Program, Hospital for Special Surgery, New York, NY 10021; and [e]Department of Pediatrics, Program in Immunology, Stanford University, Stanford, CA 94305-5164

Edited by Anjana Rao, Sanford Consortium for Regenerative Medicine and La Jolla Institute for Allergy and Immunology, La Jolla, CA, and approved November 10, 2015 (received for review June 9, 2015)

Phospholipase C gamma-2 (PLCγ2)-dependent calcium (Ca^{2+}) oscillations are indispensable for nuclear factor of activated T-cells, cytoplasmic 1 (NFATc1) activation and downstream gene transcription driving osteoclastogenesis during skeletal remodeling and pathological bone loss. Here we describe, to our knowledge, the first known function of transmembrane protein 178 (Tmem178), a PLCγ2 downstream target gene, as a critical modulator of the NFATc1 axis. In surprising contrast to the osteopetrotic phenotype of PLCγ2$^{-/-}$ mice, Tmem178$^{-/-}$ mice are osteopenic in basal conditions and are more susceptible to inflammatory bone loss, owing to enhanced osteoclast formation. Mechanistically, Tmem178 localizes to the ER membrane and regulates RANKL-induced Ca^{2+} fluxes, thus controlling NFATc1 induction. Importantly, down-regulation of Tmem178 is observed in human CD14^{+} monocytes exposed to plasma from systemic juvenile idiopathic arthritis patients. Similar to the mouse model, reduced Tmem178 expression in human cells correlates with excessive osteoclastogenesis. In sum, these findings identify an essential role for Tmem178 to maintain skeletal mass and limit pathological bone loss.

Tmem178 | osteoclasts | NFATc1 | calcium | sJIA

In recent years, the skeleton has been appreciated as a dynamic system that, in addition to serving its evident mechanical functions, cross-talks with the endocrine, nervous, immune, reproductive, and digestive systems. Skeletal fragility is observed in inflammatory, endocrine, and metabolic disorders (1, 2). Perhaps the most studied inflammatory condition associated with dysregulated bone homeostasis is rheumatoid arthritis (RA). Elevated levels of inflammatory cytokines acting in concert with the osteoclastogenic factor, receptor activator of NF-κB ligand (RANKL), drive excessive osteoclast (OC) differentiation, and lead to local joint erosion and systemic bone loss (3, 4). Pathological bone loss is also observed in children with systemic juvenile idiopathic arthritis (sJIA); low bone mass and high risk fragility fractures often persist in adults who suffered from sJIA during childhood (5). Unfortunately, current therapeutics are not always successful in suppressing both the inflammatory and resorptive components of arthritic diseases, and many patients suffer progressive and irreversible joint damage even without active system disease.

OC differentiation is initiated by the binding of RANKL to its receptor RANK on the mononuclear precursors (3, 4). Downstream of RANK signaling cascades, the nuclear factor of activated T-cells, cytoplasmic 1 (NFATc1) is required for osteoclastogenesis and directly regulates many genes important for OC differentiation and function (6–10). NFATc1 activation is primarily regulated by calcium (Ca^{2+}). RANK signaling activates the catalytic activity of phospholipase C gamma-2 (PLCγ2) to generate the second messengers inositol-1,4,5-triphosphate (IP_3) and diacylglycerol (11). IP_3, in turn, binds the IP_3 receptors (IP_3R) on the endoplasmic reticulum (ER), activating release of Ca^{2+} from the ER and consequent influx of Ca^{2+} from the extracellular milieu (12). The resulting rise in cytoplasmic Ca^{2+} and ongoing Ca^{2+} fluxes trigger the Ca^{2+}/calmodulin-dependent pathway of NFATc1 nuclear translocation to drive osteoclastogenesis (13). Targeted deletion of PLCγ2 in mice results in osteopetrosis due to insufficient NFATc1 expression. Similarly, genetic or pharmacological interference of ER or plasma membrane Ca^{2+} channel activity blocks osteoclastogenesis in vitro and in vivo by impairing NFATc1 expression (14–19). Differently from T cells, however, NFATc1 activation must be sustained throughout osteoclastogenesis over the course of days and depends on both amplitude and duration of the Ca^{2+} fluxes. For this reason, Ca^{+} mobilization must be finely controlled by regulatory proteins that potentiate or suppress Ca^{2+} transport (20, 21). However, such modulatory proteins in primary OCs are largely uncharacterized.

In this study, we report that Tmem178 is a novel PLCγ2-dependent protein that controls Ca^{2+} fluxes in the OC. In contrast to the proosteoclastogenic role of PLCγ2, however, Tmem178 negatively regulates osteoclastogenesis in vitro and in vivo. Mechanistically, Tmem178 deficiency enhances RANKL-induced Ca^{2+} oscillations, thereby increasing NFATc1 levels and osteoclastogenesis. Further highlighting the clinical relevance of our findings, human monocytes treated with plasma from sJIA patients down-regulate Tmem178 and undergo more robust

Significance

Excessive osteoclast (OC) activation and joint erosion are often observed in arthritis patients, including children suffering from systemic juvenile idiopathic arthritis (sJIA), even in the absence of active systemic symptoms. Herein, we identify a previously uncharacterized protein, transmembrane protein 178 (Tmem178), as a novel downstream target of the receptor activator of NF-κB ligand/phospholipase C gamma-2 signaling axis in the OC. Surprisingly, Tmem178 functions as a negative regulator of OC differentiation in basal and inflammatory conditions by controlling NFATc1 induction via modulation of Ca^{2+} fluxes. Importantly, Tmem178 is dysregulated in the context of sJIA, where defective Tmem178 expression is associated with enhanced OC differentiation and erosive disease. These findings represent a novel mechanism of negative feedback that limits osteoclastogenesis and consequent resorptive activity to maintain skeletal integrity.

Author contributions: C.E.D. and R.F. designed research; C.E.D., Z.Y., R.R., K.-H.P.-M., and C.M. performed research; C.M. and E.D.M. contributed new reagents/analytic tools; C.E.D., Z.Y., D.V.N., and R.F. analyzed data; C.E.D. and R.F. wrote the paper; and E.D.M. contributed to the design, analysis, and discussion of the sJIA experiments.

The authors declare no conflict of interest.

This article is a PNAS Direct Submission.

[1]To whom correspondence should be addressed. Email: faccior@wustl.edu.

This article contains supporting information online at www.pnas.org/lookup/suppl/doi:10.1073/pnas.1511285112/-/DCSupplemental.

osteoclastogenesis, suggesting that Tmem178 may be a modulator of disease-associated bone erosion.

Results

Tmem178 Deletion Decreases Bone Mass in Basal Conditions. We have reported that ablation of PLCγ2 results in a blockade of osteoclastogenesis owing to defective NFATc1 induction (11, 22). PLCγ2-deficient mice are osteopetrotic and are also protected from inflammatory osteolysis (23, 24). Therefore, we sought to identify novel PLCγ2-dependent signaling mediators that could inform therapeutic design for disorders caused by OC overactivity, such as osteoporosis and RA. We performed a gene array comparing adherent wild-type (WT) and PLCγ2-deficient OC precursors and found that Tmem178 was highly expressed in WT cells, but not in cells lacking PLCγ2 (Fig. S1*A*).

Tmem178 is a previously unstudied multipass integral membrane protein. Despite its name, Tmem178 does not share any structural domains or homology with other "Tmem" proteins. We began by assessing Tmem178 expression in whole tissues from WT and PLCγ2$^{-/-}$ mice. Strikingly, Tmem178 is highly expressed in WT whole bone, whereas transcript levels are low in other tissues including spleen, liver, thymus, and testes (Fig. 1*A*). Confirming the gene array data, Tmem178 expression strongly depends on PLCγ2. Thus, we hypothesized that Tmem178 is a downstream target controlling PLCγ2's effects on bone homeostasis.

To establish the physiological importance of Tmem178, we examined the bone phenotype of Tmem178-null mice. We expected Tmem178$^{-/-}$ mice to mirror the osteopetrotic phenotype of PLCγ2$^{-/-}$ mice. Surprisingly, 16-wk-old female Tmem178$^{-/-}$ mice display a 35% decrease in trabecular bone volume with significant trabecular thinning compared with WT littermates (Fig. 1 *B–D*). Tartrate-resistant acid phosphatase (TRAP) staining of long bone sections reveals a significant increase in OC surface normalized to bone surface in Tmem178$^{-/-}$ mice (Fig. 1 *E* and *F*), wheres osteoblast (OB) numbers are equivalent between genotypes (Fig. S1*B*). Accordingly, mineral apposition rate (MAR), bone formation rate (BFR), and RANKL and OPG mRNA levels in whole bones flushed of marrow cells are similar in the two genotypes (Fig. S1 *C–G*). These in vivo data suggest that Tmem178 suppresses OC differentiation via an unexpected negative feedback loop downstream of PLCγ2.

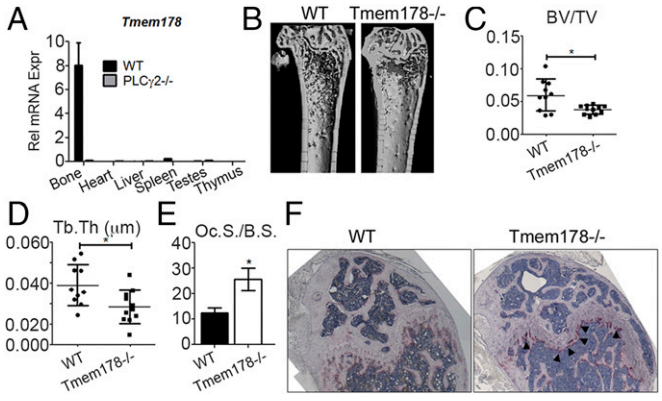

Fig. 1. Deletion of Tmem178 decreases bone mass in basal conditions. (*A*) Quantitative RT-PCR (Q-RT PCR) analysis of Tmem178 mRNA in whole tissues from WT or PLCγ2$^{-/-}$ mice. (*B*) Representative microCT images of the proximal femurs of 16-wk-old female WT and Tmem178$^{-/-}$ mice. WT $n = 10$, Tmem178$^{-/-}$ $n = 11$. (*C*) Trabecular bone volume per tissue volume (BV/TV) quantified from microCT shown in *B*. *$P < 0.05$. (*D*) Trabecular thickness (Tb.Th.) from microCT in *B*. *$P < 0.05$. (*E*) Quantification of OC surface per bone surface (Oc.S/B.S.) from TRAP-stained sections. $n = 5$ per genotype. *$P < 0.05$. (*F*) Representative images of TRAP-stained femurs analyzed in *E*. Arrows indicate OCs.

Tmem178 Expression Depends on PLCγ2/NFATc1 Signaling. Because the in vivo data suggested OC-intrinsic effects, we examined Tmem178 expression in OC lineage cells in vitro. Tmem178 mRNA increases during osteoclastogenesis and depends on PLCγ2 (Fig. 2*A*). A similar extent of Tmem178 induction is observed in human CD14^{+} monocytes treated with RANKL compared with M-CSF alone (Fig. 2*B*). In contrast to the OCs, Tmem178 is not significantly expressed in the OBs (Fig. S1*H*), confirming the observation that Tmem178 deletion does not affect bone formation.

Because NFATc1 is downstream of PLCγ2, and the Tmem178 promoter harbors NFAT consensus binding sites (rvista.dcode.org), we examined Tmem178 expression in NFATc1-deficient cells. We found that RANKL-induced Tmem178 up-regulation is blunted in NFATc1-null cells compared with controls (Fig. S1*I*). In addition to NFAT, PLCγ2 controls the classical NF-κB pathway following RANKL and integrin-mediated adhesion. We found that Tmem178 expression is induced by adhesion, and this increase partially depends on the classical NF-κB subunit p65 (Fig. S1*J*). These data position Tmem178 directly downstream of the RANKL/PLCγ2 axis in the OC.

Tmem178 Deletion Enhances Osteoclastogenesis. To determine the role of Tmem178 in the OC, we cultured bone marrow macrophages (BMMs) with M-CSF and RANKL for 3–5 d. Tmem178$^{-/-}$ BMMs display accelerated OC differentiation compared with WT (Fig. 2 *C* and *D*). Increased osteoclastogenesis is also observed in the coculture system with either WT or Tmem178$^{-/-}$ bone marrow stromal cells (Fig. S2*A*). Furthermore, bone resorption was significantly increased in Tmem178$^{-/-}$ cells cultured on bone for 10 d compared with WT (Fig. S2 *B* and *C*). Because enhanced resorption could be a consequence of increased OC numbers, we analyzed the resorptive capacity of individual OCs by plating committed OCs (differentiated on plastic with M-CSF and RANKL for 3 d) on bone slices for 48 h. Results show equivalent bone resorption by Tmem178$^{-/-}$ and WT OCs (Fig. S2 *D* and *E*). Altogether these findings demonstrate that Tmem178 is a negative regulator of OC differentiation but does not exert a direct effect on the cell's resorptive capacity.

Tmem178 Deficiency Enhances Ca^{2+} Fluxes in OCs. To understand how Tmem178 modulates OC differentiation, we assessed activation of RANKL-induced NF-κB and MAPKs. We find no perceptible differences in NF-κB and MAPK activation between WT and Tmem178$^{-/-}$ BMMs (*Top*) or preOCs (*Bottom*) (Fig. S3*A*). Similarly, M-CSF induction of p-AKT and p-ERK is equivalent in both genotypes (Fig. S3*B*).

Because RANK signaling to PLCγ2 activates Ca^{2+} fluxes that are indispensable for osteoclastogenesis, we measured intracellular Ca^{2+} levels in single cells by ratiometric imaging. Cells were cultured with M-CSF and RANKL for 24 h (preOCs) before loading with Fura-2AM and imaging. Tmem178$^{-/-}$ preOCs consistently show higher levels of intracellular Ca^{2+} with fluxes of greater amplitude compared with WT (Fig. 3 *A* and *B*; 10 representative cells per genotype). During osteoclastogenesis, Ca^{2+} is released from the ER, allowing store-operated Ca^{2+} entry (SOCE) from the extracellular milieu. To better understand how Tmem178 modulates Ca^{2+} fluxes, we used HEK293T cells, which display more consistent Ca^{2+} measurements than primary OCs. Ca^{2+} fluxes were detected in basal conditions, in response to thapsigargin (Tg) in Ca^{2+}-free medium to induce ER Ca^{2+} release and following addition of 1.8 mM Ca^{2+} to allow SOCE. Surprisingly, cells expressing ectopic Tmem178 show a slower and reduced ER Ca^{2+} release in response to Tg, but reach the same levels of intracellular Ca^{2+} following SOCE (Fig. 3*C*). This effect is not due to a change in total ER Ca^{2+} content, because ionomycin-induced ER Ca^{2+} emptying is similar in Tmem178-expressing cells versus controls (Fig. S4*A*).

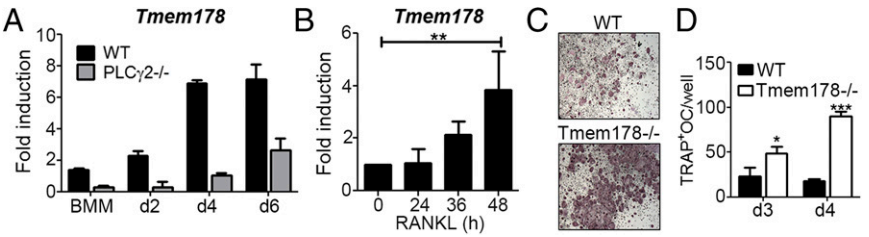

Fig. 2. Tmem178 deficiency enhances osteoclastogenesis. (*A*) Q-RT PCR analyses of Tmem178 mRNA during RANKL-induced osteoclastogenesis in WT and PLCγ2$^{-/-}$ cells. (*B*) Q-RT PCR analysis of Tmem178 mRNA in human OC cultures. $^{**}P < 0.01$. (*C*) TRAP staining of WT and Tmem178$^{-/-}$ OCs. Images are representative of more than five experiments, each performed in triplicate. (*D*) Quantification of TRAP+ OCs in *D*. $^{*}P < 0.05$, $^{***}P < 0.001$.

Tmem178 Resides in the ER and Binds to Stim1. Supporting our findings that Tmem178 acts on ER Ca^{2+} mobilization, we determined by immunofluorescence that Tmem178 localizes to the ER but not the plasma membrane in mature OCs (Fig. 3*D*). Next, we wanted to know whether Tmem178 interacts with known ER-resident proteins involved in Ca^{2+} mobilization. Inositol triphosphate receptors (IP3Rs) are ER-resident Ca^{2+} channels, which facilitate ER Ca^{2+} release and consequent intracellular Ca^{2+} fluxes in response to IP3 generated by PLCγ signaling. IP3R isoforms 1, 2, and 3 are expressed in the OC, and IP3R2 and IP3R3 modulate RANKL-stimulated Ca^{2+} fluxes (14). However, by coimmunoprecipitation, we did not detect an interaction between Tmem178 and any IP3R isoform (Fig. S4*B*).

Next we considered the protein Stim1, which is an ER Ca^{2+} sensor controlling Ca^{2+} fluxes during osteoclastogenesis (16, 17, 25). We expressed Tmem178-HA and Stim1-Myc in HEK293T cells and found that Tmem178 and Stim1 interact in resting conditions (control), and to a less extent in the presence of Tg and Tg + 1.8 mM Ca^{2+} (Fig. 3*E*). Using confocal microscopy, we confirmed Tmem178/Stim1 interaction in BMMs treated with RANKL for 24 h (Fig. S4*C*). Although Stim1 bears significant homology to the related protein Stim2, we did not detect an interaction between Tmem178 and Stim2 (Fig. S4*D*).

Because Stim1 binds to Orai1 to activate SOCE, we coexpressed Tmem178, Stim1, and Orai1 in HEK293T cells. We found no interaction between Tmem178 and Orai1, nor did we find that the presence or absence of Tmem178 affects Stim1 coupling to Orai1 (Fig. 3 *E* and *F*) in resting conditions or following Tg and 1.8 mM Ca^{2+}. These data indicate that Tmem178 binds to Stim1 independent of SOCE.

Tmem178 Negatively Regulates OC Formation by Controlling NFATc1. Based on the increase in Ca^{2+} fluxes in Tmem178$^{-/-}$ cells, we hypothesized that amplified NFATc1 levels may underlie enhanced OC formation in the absence of Tmem178. Indeed, Tmem178$^{-/-}$ cultures show heightened NFATc1 transcript levels throughout osteoclastogenesis (Fig. 4*A*) and a higher percentage of cells with NFATc1 nuclear staining (Fig. 4*B* and Fig. S5*A*). Consistent with increased NFATc1 nuclear levels, we observed an earlier and greater magnitude of induction of NFATc1 target genes including TRAP (*Acp5*), Cathepsin K (*CtsK*), and calcitonin receptor (*Calcr*) (Fig. 4*C*). Cytoplasmic and nuclear fractionation of RANKL-treated cells also illustrates earlier and sustained NFATc1 nuclear

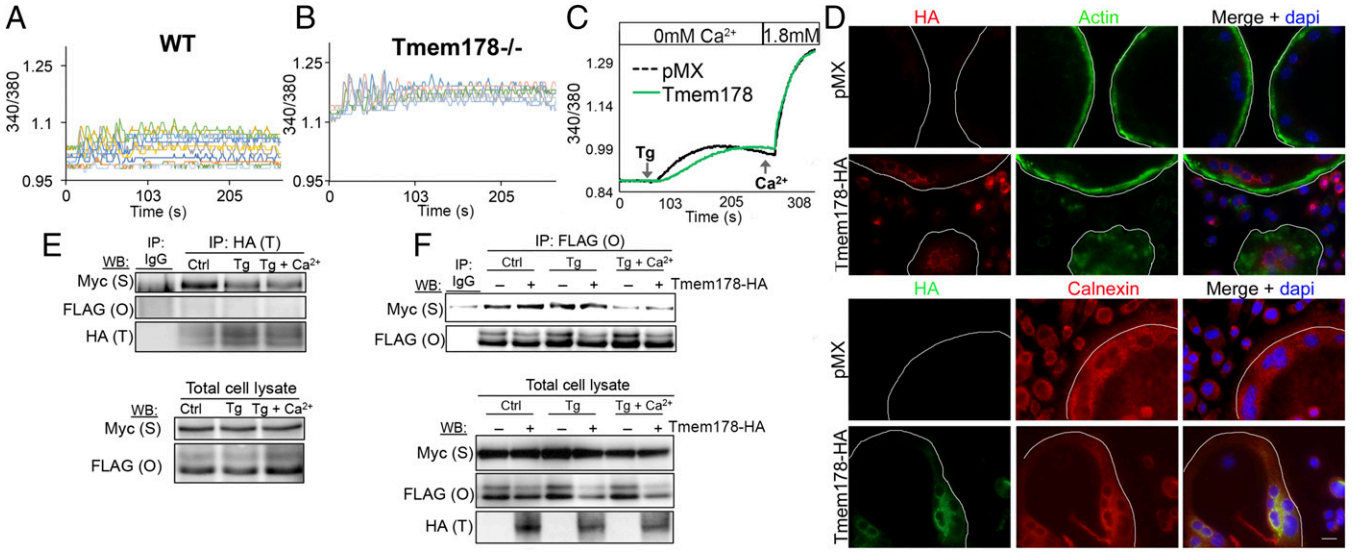

Fig. 3. Tmem178 is an ER-resident protein that targets RANKL/Ca^{2+} signaling. (*A*) Cytosolic Ca^{2+} measurements in WT preOCs. Ten representative cells are shown, representative of more than four independent experiments. (*B*) Cytosolic Ca^{2+} measurements in Tmem178$^{-/-}$ preOC as in *A*. (*C*) Ratiometric imaging of HEK293T cells expressing empty vector pMX or Tmem178-HA cultured in Ca^{2+} free-HBSS and stimulated with 1 μM Tg, or Tg + 1.8 mM Ca^{2+}. Traces are the average of more than 40 cells per condition, representative of three experiments. (*D*) Localization of Tmem178 in mature OCs by immunofluorescence. Phalloidin is used as plasma membrane marker, calnexin as an ER marker, and DAPI as a nuclear stain. (Scale bar: 100 μm.) Manually contoured white line denotes cell edge. (*E*) HEK293T cells transfected with Tmem178-HA (T), Stim1-Myc-His (S), and Orai1-FLAG (O) were untreated, stimulated for 10 min with 1 μM Tg in Ca^{2+}-free media, or treated with Tg followed by the addition of extracellular Ca^{2+} as indicated. Lysates were immunoprecipitated and blotted as labeled. Representative of more than 10 experiments. (*F*) HEK293T cells transfected with Stim1-Myc-His and Orai1-FLAG with or without Tmem178-HA and treated as in *E*. Total cell lysates show ectopic protein expression. Representative of more than 10 experiments.

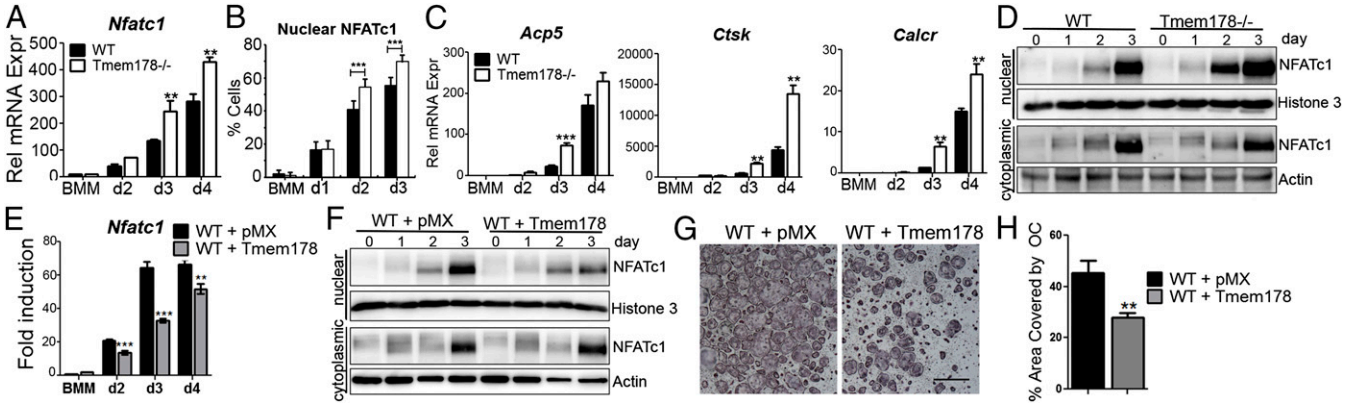

Fig. 4. Tmem178 controls RANKL-induced NFATc1 activation. (*A*) Q-RT PCR analysis of NFATc1 during osteoclastogenesis. $^{**}P < 0.01$. (*B*) Quantification of NFATc1 nuclear localization. Data are pooled from two independent experiments, 3–9 coverslips/condition per experiment. $^{***}P < 0.001$. (*C*) Q-RT PCR analysis of osteoclastogenic markers in WT and Tmem178$^{-/-}$ cells during osteoclastogenesis. Acp5, TRAP; Calcr, Calcitonin receptor; Ctsk K, Cathepsin K. $^{**}P < 0.01$, $^{***}P < 0.001$. (*D*) Western blot analysis of NFATc1 nuclear translocation in response to RANKL in WT and Tmem178$^{-/-}$ OCs for the indicated days of culture. Histone 3 and actin are shown as nuclear and cytoplasmic loading controls, respectively. Representative of three experiments. (*E*) Q-RT PCR analysis of NFATc1 mRNA during osteoclastogenesis in WT cells expressing pMX or Tmem178-HA. $^{**}P < 0.01$, $^{***}P < 0.001$. (*F*) Western blot analysis of NFATc1 as in *D* in pMX and Tmem178-expressing cells. Representative of three experiments. (*G*) Representative images of TRAP^{+} OCs expressing pMX or Tmem178-HA. (*H*) Quantification of percent area covered by OCs in *G*. $^{**}P < 0.01$.

translocation in Tmem178$^{-/-}$ OCs compared with WT (Fig. 4*D* and Fig. S5*B*).

To determine whether Tmem178 suppresses osteoclastogenesis by limiting NFATc1 levels, we ectopically expressed Tmem178 in WT BMMs and analyzed their ability to induce NFATc1 and undergo OC differentiation. Tmem178 expression attenuates NFATc1 transcripts and reduces NFATc1 nuclear translocation in response to RANKL (Fig. 4 *E* and *F* and Fig. S5*C*), with a resulting reduction in osteoclastogenesis (Fig. 4 *G* and *H*). Altogether, these data indicate that Tmem178 acts in a negative feedback loop to restrain further NFATc1 activation and OC differentiation.

Tmem178$^{-/-}$ Mice Suffer Profound Inflammatory Osteolysis. Next, we wondered whether Tmem178 similarly regulates OC formation driven by inflammatory cytokines. Addition of TNF-α or LPS further exacerbates Tmem178$^{-/-}$ OC differentiation in vitro (Fig. 5*A*). Most importantly, Tmem178$^{-/-}$ mice injected with LPS over the calvaria develop profound focal osteolysis (Fig. 5 *B* and *C*), and increased OC surface compared with WT (Fig. 5*D* and Fig. S6*A*).

To determine whether Tmem178 could modulate bone loss in a model of inflammatory arthritis, WT and Tmem178$^{-/-}$ mice were injected with arthritogenic serum from K/BxN mice. Both genotypes develop an equivalent inflammatory response, measured by paw thickness (Fig. S6*B*). However, Tmem178$^{-/-}$ mice suffer significantly more bone loss, measured by remaining bone volume at the knee by microCT (Fig. 5 *E* and *F*), driven by a significant increase in OC differentiation (Fig. 5*G*). Altogether these data indicate that Tmem178 restrains inflammatory bone loss.

Tmem178 Is Down-Regulated in Human Monocytes Exposed to sJIA Plasma. Based on the above observations, we wondered whether changes in Tmem178 levels would be detected in patients affected by inflammatory bone loss, such as sJIA. Seminal studies of sJIA pathogenesis proved that circulating factors present in the plasma of patients are sufficient to drive the disease phenotype even in healthy monocytes (26, 27). We cultured CD14^{+} monocytes from healthy donors with M-CSF and RANKL for 2 d to generate preOCs and then added the plasma collected from healthy controls (HC) ($n = 10$) or sJIA patients ($n = 20$). Strikingly, Tmem178 transcript is significantly reduced in CD14^{+} cells treated with sJIA plasma compared with HC plasma (Fig. 5*H*). The addition of sJIA plasma potently augments OC differentiation (Fig. 5 *I* and *J*). Notably, Tmem178 expression is further blunted, whereas OC numbers are significantly increased, following exposure to plasma from five patients with erosive disease (Fig. 5 *I* and *J*). Finally, we tested the ability of sJIA plasma to affect osteoclastogenesis in murine cells expressing ectopic Tmem178 or control pMX empty vector. As expected, osteoclastogenesis is enhanced in pMX cells treated with sJIA plasma compared with HC plasma (Fig. 5*K*). Most importantly, ectopic expression of Tmem178 in cells exposed to sJIA plasma is sufficient to overcome excessive OC differentiation, returning to the HC baseline. Taken together, these data indicate that defective Tmem178 expression may drive excessive osteoclastogenesis and contribute to erosive disease in sJIA.

Discussion

As the sole bone-resorbing cell in the body, the OC must be carefully regulated to allow for healthy skeletal remodeling, respond to physiological stress, and return to homeostasis. Activation and termination of the signaling pathways underlying the formation of mature OCs from mononuclear precursors is a critical checkpoint of control. Here we identify a role for Tmem178 as a previously identified target of the RANKL/PLCγ2 pathway; in turn, Tmem178 acts in a negative feedback loop to restrain NFATc1 and excessive OC differentiation in mice and humans. This work expands the understanding of cell-intrinsic negative feedback mechanisms that are necessary to maintain healthy bone and identifies Tmem178 as a new negative regulator of RANKL-induced Ca^{2+} fluxes.

Because of the importance of Ca^{2+} amplitude and duration in discriminating between different response pathways, cytoplasmic Ca^{2+} levels are tightly regulated. Regulators of Ca^{2+} channel activity in the OC have only recently come under investigation. Ong et al. described the importance of transient receptor potential cation channel 1 in SOCE activation during OC formation (28). Similarly, Tmem64 (no homology to Tmem178) promotes RANKL-induced Ca^{2+} oscillations by bolstering the activity of Sarco-Endoplasmic Reticulum ATPase isoform 2, which actively refills ER Ca^{2+} stores, and is required for NFATc1 induction and osteoclastogenesis (15, 19, 29). Whereas these studies demonstrate that the loss of positive regulators of Ca^{2+} fluxes perturbs osteoclastogenesis and leads to increased bone mass, we now identify a negative regulator of Ca^{2+} fluxes whose ablation leads to up-regulation of NFATc1 levels and an osteopenic phenotype.

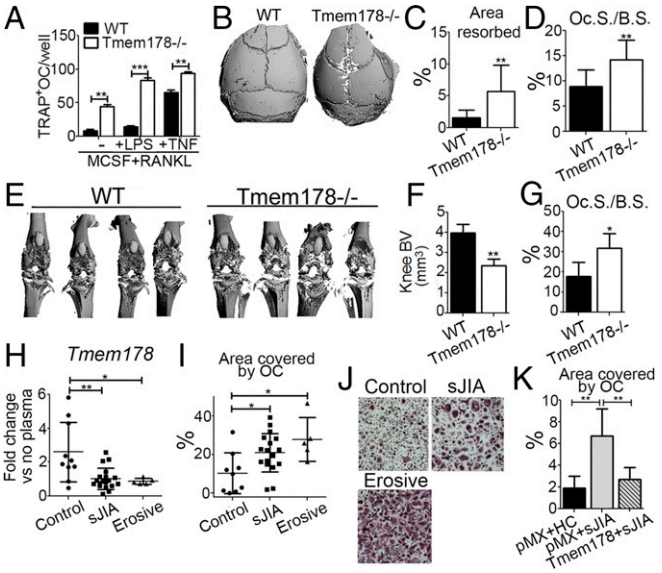

Fig. 5. Tmem178 deletion worsens inflammatory bone loss. (*A*) Quantification of TRAP$^+$ OCs in WT and Tmem178$^{-/-}$ cells following the addition of 100 ng/mL LPS or 10 ng/mL TNF-α on day 2 of OC culture. ***$P < 0.001$, **$P < 0.01$. (*B*) Representative microCT 3D reconstructions of calvaria from WT and Tmem178$^{-/-}$ mice receiving 100 μg of supracalvarial LPS. $n = 10$ per genotype. (*C*) Quantification of the percent area resorbed on the calvaria from *B*. **$P < 0.01$. (*D*) Quantification of OC surface per bone surface (Oc.S./B.S.) in *B*. **$P < 0.01$. (*E*) Representative microCT 3D reconstructions of knees from WT and Tmem178$^{-/-}$ mice after K/BxN serum transfer arthritis. $n = 10$ per genotype. (*F*) Quantification of bone volume remaining at the knee in mice in *E*. **$P < 0.01$, $n = 10$ per genotype. (*G*) Quantification of Oc.S/B.S. from *E*. **$P < 0.01$, $n = 10$ per genotype. (*H*) Q-RT PCR analysis of Tmem178 mRNA expression in human CD14$^+$ cells cultured in osteoclastogenic medium for 2 d before addition of healthy control (HC) or sJIA plasma. **$P < 0.01$, *$P < 0.05$. (*I*) Quantification of area covered by TRAP + OCs cultured with HC plasma or sJIA plasma. *$P < 0.05$. Triplicate wells were counted. Representative of two independent experiments. (*J*) Representative images of TRAP$^+$ OCs in *I*. (*K*) Quantification of OC area from murine BMMs expressing pMX or Tmem178 and treated with HC or sJIA plasma. **$P < 0.01$.

NFAT proteins show enhanced Ca^{2+} sensitivity compared with other transcription factors, enabling NFAT transcription by low Ca^{2+} levels (30). Furthermore, in the OC, differently from other cell types such as T cells, not only the amplitude of Ca^{2+} signaling but also the generation of continuous Ca^{2+} oscillations in response to RANKL is required for efficient NFATc1 transcriptional activation. We find that following RANKL exposure, Tmem178$^{-/-}$ cells reach higher intracellular Ca^{2+} levels compared with WT, which correlate with greater NFATc1 induction and increased NFATc1 nuclear translocation. Consequently, Tmem178$^{-/-}$ cells undergo more rapid and robust osteoclastogenesis in vitro and in vivo, and Tmem178$^{-/-}$ mice develop osteopenia. In contrast, ectopic Tmem178 expression in OC precursors reduces NFATc1 levels and decreases osteoclastogenesis in physiological conditions and following exposure to sJIA plasma.

Stim1 is an ER Ca^{2+} sensor expressed in numerous cell types, including OCs, mast cells, B cells, and T cells. Pharmacological inhibition of Stim1 impairs SOCE, thereby blocking osteoclastogenesis (16). In addition to associating with Orai1 to control SOCE, Stim1 also couples to numerous other Ca^{2+} channels, Ca^{2+} pumps, ER chaperone proteins, and regulatory adaptor proteins, thereby influencing multiple pathways of Ca^{2+} transport (31). In kidney epithelial cells, Stim1 interacts with polycystin-1, diminishing IP3R-mediated ER Ca^{2+} release (32). In aortic endothelial cells, Stim1 potentiates IP3R-mediated ER Ca^{2+} release (33). In muscle cells, Stim1 inhibits Ca^{2+} discharge from the sarcoplasmic reticulum (34). Differences in ER Ca^{2+} release were also noted in Stim1$^{-/-}$ mast cells in response to antigen or Tg (35). Thus, Stim1 has a critical role not only in sensing ER Ca^{2+} levels and activating SOCE, but also appears to regulate, at least in part, ER Ca^{2+} release in multiple cell types. In the OC, we find that Tmem178 localizes to the ER where it associates with Stim1. Interestingly, Tmem178 does not bind to Orai1 or inhibit Orai1-Stim1 coupling, and Tmem178 does not modulate SOCE. Instead, Tmem178 ectopic expression reduces Tg-mediated ER Ca^{2+} release, suggesting that Tmem178 may modulate Stim1's roles independent of SOCE. Further studies are necessary to wholly understand the mechanism of Tmem178-mediated Ca^{2+} regulation and the significance of the Tmem178–Stim1 complex during osteoclastogenesis.

Tmem178 interaction with Stim1 is particularly interesting in the context of arthritis. Stim1 single nucleotide polymorphisms (SNPs) were recently identified in patients with ankylosing spondylitis (AS), a chronic inflammatory disease of the spine and joints (36). These SNPs correlated with significantly higher inflammatory markers including C-reactive protein and in some cases higher circulating levels of TNF-α and IL-6. Although we did not have access to AS patient samples to measure Tmem178 levels or Tmem178/Stim1 binding, we found that reduced Tmem178 expression is associated with augmented osteoclastogenesis in the context of sJIA. Further supporting a role for Tmem178 in inflammatory arthritis, Tmem178$^{-/-}$ mice suffer profound osteolysis following LPS and in K/BxN arthritis, and in vitro studies show increased responsiveness to TNF-induced osteoclastogenesis. These results strongly indicate that Tmem178 acts in a negative feedback loop to restrain exuberant osteoclastogenesis and regulate bone mass in basal and inflammatory conditions.

sJIA is characterized by arthritis and systemic inflammation. Bone erosion and systemic bone loss were observed in up to 50% of children with sJIA in the prebiologic era. Even more recently, CARRAnet registry data (collected since 2010) on 435 children with sJIA show that joint damage remains a significant problem for at least 20% of these patients despite remission of the systemic inflammation. To date, there are no markers that identify the subset of sJIA patients who will develop erosive disease. Further, the diagnosis of sJIA is a clinical diagnosis of exclusion, and unfortunately a delayed diagnosis contributes to the development of erosive changes. We now show that Tmem178 expression is significantly reduced in human CD14$^+$ monocytes exposed to sJIA plasma, whereas OC differentiation is increased. Most importantly, ectopic expression of Tmem178 restrains the increase in OC formation induced by sJIA plasma. Consistent with this result, we observe a significant reduction in Tmem178 levels in samples treated with plasma from sJIA patients with erosive disease, positioning Tmem178 as a potential biomarker for the subset of sJIA patients who will develop erosive disease. These initial findings with a limited number of patient samples necessitate future investigations with larger cohorts of sJIA patients. We also do not yet understand the complex upstream mechanism that regulates Tmem178 expression in response to sJIA plasma. Further investigation into the role of Tmem178 in the pathogenesis of sJIA and other arthritic conditions associated with erosive disease is warranted.

In conclusion, we have identified Tmem178 as a new PLCγ2-dependent gene. Despite its dependence on the RANKL/PLCγ2 pathway, however, Tmem178 acts in a negative feedback loop to restrain NFATc1 up-regulation and OC responses in basal and pathological conditions.

Methods and Materials

Mice. PLCγ2$^{-/-}$ mice were kindly provided by J. N. Ihle, St. Jude Children's Research Hospital, Memphis, TN. Tmem178$^{-/-}$ mice (Strain B6;129S5-Tmem178tm1Lex/Mmucd) were generated by the trans-NIH Knock-Out Mouse Project (KOMP) and purchased from the KOMP Repository at University of California Davis (https://www.komp.org) (stock no. 032664-UCD). Tmem178 bone phenotyping was performed with mice of the C57BL/6–129

background maintained by heterozygous breeding. In vitro experiments were repeated with bone marrow from both mice of C57BL/6–129 and C57BL/6 background. Analysis of bone phenotype by microCT and histology was performed as described (37). All experiments were approved by the Washington University School of Medicine animal care and use committee.

Primary Cell Culture. BMMs were isolated from 6- to 8-wk-old mice as described (11). To form OCs, BMMs were cultured with 50 ng/mL GST-RANKL and 10 ng/mL M-CSF (osteoclastogenic medium) for 3–5 d. Cells were fixed in 4% (vol/vol) paraformaldehyde in PBS (Polysciences) and stained for TRAP by using the leukocyte acid phosphatase kit (Sigma).

Plasmids and Retrovirus Generation. Human Tmem178 cDNA (clone ID 528607; Open Biosystems) was cloned into the blasticidin-resistant pMX retroviral vector containing an HA tag at the C terminus by using BamHI and XhoI restriction sites. Stim1-Myc and Orai1-FLAG were gifts from Monika Vig, Washington University in St. Louis, St. Louis.

Single-Cell Ca^{2+} Measurements. Cells were loaded with 3 μM Fura-2AM (Invitrogen) in phenol red-free DMEM (Invitrogen) containing 10 ng/mL M-CSF for 30 min at room temperature in the dark and imaged immediately in phenol red-free DMEM containing 10 ng/mL M-CSF and 100 ng/mL RANKL. Fura-2 ratios were measured by alternate excitation at 340 nm and 380 nm at a frequency of 1 image pair every 2 s. At least 40 cells per field were analyzed in each replicate.

Human Plasma Preparation and Osteoclastogenesis. All subjects provided informed consent before participating in the study in accordance with the Declaration of Helsinki. Plasma was prepared from whole, anticoagulated blood within 2 h after blood draw. $CD14^+$ PBMCs were isolated from healthy donor by Ficoll gradient centrifugation followed by positive selection with anti-CD14 magnetic beads (Miltenyi Biotec). For osteoclastogenesis, 15% plasma by volume was added to $CD14^+$ cells after 2 d of culture with 15 ng/mL hM-CSF and 100 ng/mL GST-RANKL. For Tmem178 mRNA analysis, $CD14^+$ preOCs were incubated with 15% control or patient plasma for 8 h before mRNA extraction.

Study Approval. For all mouse studies, experiments were approved by the Washington University School of Medicine animal care and use committee. Human studies were approved by the Institutional Review Board at Stanford University.

Statistics. All data represent mean ± SD. Data were analyzed by using two-tailed Student's *t* test. Time course experiments were analyzed by using a one-way ANOVA followed by a post hoc Newman–Keuls test of significance. *P* values are indicated where applicable.

Detailed materials and methods are available in the *SI Materials and Methods*.

ACKNOWLEDGMENTS. We thank Dr. A. Aliprantis and Dr. J. Charles for providing $NFATc1^{fl/fl}$ bone marrow, Dr. J. Warren for assistance with molecular cloning, and Dr. K. Hyrc for assistance with Ca^{2+} and confocal imaging. This work was supported by a Children's Discovery Institute at Washington University School of Medicine (WUSM) Grant (to R.F. and D.N.), NIH Grants R01 AR053628 and AR066551 (to R.F.), and Shriners Hospital Grant 85100 (to R.F.). D.V.N. was supported by NIH Grant R01 AR052705. C.M. and E.D.M. were supported by NIH Grant R01 AR061297 and by the Great West Region, Arthritis Foundation, University of California, San Francisco-Stanford University Center of Excellence for Arthritis Research. K.-H.P.-M. was supported by NIH Grant AR061430. MicroCT and histology were supported by The Washington University Musculoskeletal Research Center, funded by NIH Grant P30 AR057235. Ca^{2+} and confocal imaging were supported by the Hope Center Alafi Neuroimaging Lab and the Center for Investigation of Membrane Excitability Diseases Live Cell Imaging Facility at WUSM. C.D. was supported by the Metabolic Skeletal Disorders Training Grant T32 AR060719-01.

1. Karsenty G, Ferron M (2012) The contribution of bone to whole-organism physiology. *Nature* 481(7381):314–320.
2. DiGirolamo DJ, Clemens TL, Kousteni S (2012) The skeleton as an endocrine organ. *Nat Rev Rheumatol* 8(11):674–683.
3. Lacey DL, et al. (1998) Osteoprotegerin ligand is a cytokine that regulates osteoclast differentiation and activation. *Cell* 93(2):165–176.
4. Boyle WJ, Simonet WS, Lacey DL (2003) Osteoclast differentiation and activation. *Nature* 423(6937):337–342.
5. Thornton J, et al. (2011) Bone health in adult men and women with a history of juvenile idiopathic arthritis. *J Rheumatol* 38(8):1689–1693.
6. Ishida N, et al. (2002) Large scale gene expression analysis of osteoclastogenesis in vitro and elucidation of NFAT2 as a key regulator. *J Biol Chem* 277(43):41147–41156.
7. Asagiri M, et al. (2005) Autoamplification of NFATc1 expression determines its essential role in bone homeostasis. *J Exp Med* 202(9):1261–1269.
8. Takayanagi H, et al. (2002) Induction and activation of the transcription factor NFATc1 (NFAT2) integrate RANKL signaling in terminal differentiation of osteoclasts. *Dev Cell* 3(6):889–901.
9. Crotti TN, et al. (2008) PU.1 and NFATc1 mediate osteoclastic induction of the mouse beta3 integrin promoter. *J Cell Physiol* 215(3):636–644.
10. Aliprantis AO, et al. (2008) NFATc1 in mice represses osteoprotegerin during osteoclastogenesis and dissociates systemic osteopenia from inflammation in cherubism. *J Clin Invest* 118(11):3775–3789.
11. Mao D, Epple H, Uthgenannt B, Novack DV, Faccio R (2006) PLCgamma2 regulates osteoclastogenesis via its interaction with ITAM proteins and GAB2. *J Clin Invest* 116(11):2869–2879.
12. Putney JW, Jr (2005) Capacitative calcium entry: Sensing the calcium stores. *J Cell Biol* 169(3):381–382.
13. Negishi-Koga T, Takayanagi H (2009) Ca2+-NFATc1 signaling is an essential axis of osteoclast differentiation. *Immunol Rev* 231(1):241–256.
14. Kuroda Y, Hisatsune C, Nakamura T, Matsuo K, Mikoshiba K (2008) Osteoblasts induce Ca2+ oscillation-independent NFATc1 activation during osteoclastogenesis. *Proc Natl Acad Sci USA* 105(25):8643–8648.
15. Yang YM, et al. (2009) Alteration of RANKL-induced osteoclastogenesis in primary cultured osteoclasts from SERCA2+/- mice. *J Bone Miner Res* 24(10):1763–1769.
16. Zhou Y, et al. (2011) The role of calcium release activated calcium channels in osteoclast differentiation. *J Cell Physiol* 226(4):1082–1089.
17. Hwang SY, Putney JW (2012) Orai1-mediated calcium entry plays a critical role in osteoclast differentiation and function by regulating activation of the transcription factor NFATc1. *FASEB J* 26(4):1484–1492.
18. Kuroda Y, et al. (2012) Cot kinase promotes Ca2+ oscillation/calcineurin-independent osteoclastogenesis by stabilizing NFATc1 protein. *Mol Cell Biol* 32(14):2954–2963.
19. Kim H, et al. (2013) Tmem64 modulates calcium signaling during RANKL-mediated osteoclast differentiation. *Cell Metab* 17(2):249–260.
20. Choe CU, Ehrlich BE (2006) The inositol 1,4,5-trisphosphate receptor (IP3R) and its regulators: Sometimes good and sometimes bad teamwork. *Sci STKE* 2006(363):re15.
21. Srikanth S, Gwack Y (2012) Orai1, STIM1, and their associating partners. *J Physiol* 590(Pt 17):4169–4177.
22. Decker C, Hesker P, Zhang K, Faccio R (2013) Targeted inhibition of phospholipase C γ2 adaptor function blocks osteoclastogenesis and protects from pathological osteolysis. *J Biol Chem* 288(47):33634–33641.
23. Cremasco V, Graham DB, Novack DV, Swat W, Faccio R (2008) Vav/Phospholipase Cgamma2-mediated control of a neutrophil-dependent murine model of rheumatoid arthritis. *Arthritis Rheum* 58(9):2712–2722.
24. Cremasco V, et al. (2010) Phospholipase C gamma 2 is critical for development of a murine model of inflammatory arthritis by affecting actin dynamics in dendritic cells. *PLoS One* 5(1):e8909.
25. Hwang SY, et al. (2012) Deletion of Orai1 alters expression of multiple genes during osteoclast and osteoblast maturation. *Cell Calcium* 52(6):488–500.
26. Nguyen KD, et al. (2011) Serum amyloid A overrides Treg anergy via monocyte-dependent and Treg-intrinsic, SOCS3-associated pathways. *Blood* 117(14):3793–3798.
27. Nguyen KD, et al. (2014) Serum amyloid A induces mitogenic signals in regulatory T cells via monocyte activation. *Mol Immunol* 59(2):172–179.
28. Ong EC, et al. (2013) A TRPC1 protein-dependent pathway regulates osteoclast formation and function. *J Biol Chem* 288(31):22219–22232.
29. Feske S (2007) Calcium signalling in lymphocyte activation and disease. *Nat Rev Immunol* 7(9):690–702.
30. Dolmetsch RE, Lewis RS, Goodnow CC, Healy JI (1997) Differential activation of transcription factors induced by Ca2+ response amplitude and duration. *Nature* 386(6627):855–858.
31. Soboloff J, Rothberg BS, Madesh M, Gill DL (2012) STIM proteins: Dynamic calcium signal transducers. *Nat Rev Mol Cell Biol* 13(9):549–565.
32. Santoso NG, Cebotaru L, Guggino WB (2011) Polycystin-1, 2, and STIM1 interact with IP(3)R to modulate ER Ca release through the PI3K/Akt pathway. *Cell Physiol Biochem* 27(6):715–726.
33. Béliveau É, Lessard V, Guillemette G (2014) STIM1 positively regulates the Ca2+ release activity of the inositol 1,4,5-trisphosphate receptor in bovine aortic endothelial cells. *PLoS One* 9(12):e114718.
34. Lee KJ, et al. (2013) STIM1 negatively regulates Ca^{2+} release from the sarcoplasmic reticulum in skeletal myotubes. *Biochem J* 453(2):187–200.
35. Baba Y, et al. (2008) Essential function for the calcium sensor STIM1 in mast cell activation and anaphylactic responses. *Nat Immunol* 9(1):81–88.
36. Wei JC, et al. (2012) Genetic polymorphisms of stromal interaction molecule 1 associated with the erythrocyte sedimentation rate and C-reactive protein in HLA-B27 positive ankylosing spondylitis patients. *PLoS One* 7(12):e49698.
37. Cremasco V, et al. (2012) Protein kinase C-delta deficiency perturbs bone homeostasis by selective uncoupling of cathepsin K secretion and ruffled border formation in osteoclasts. *J Bone Miner Res* 27(12):2452–2463.